Journal of the Serbian Society for Computational Mechanics / Vol. 6 / No. 2, 2012 / pp. 145-159

(UDC: 611.018.63:537.63)

Analytical and numerical analysis of magnetic separation of cardiomyocytes

B.Cirkovic[1],V.Isailovic[2], Z.Milosevic[2], J.Radulovic[1], A.Sofla[3], M.Radisic[3], M.Kojic[2,4], N.Filipovic[1,2]

[1] Faculty of Engineering, University of Kragujevac, Kragujevac, Serbia
[2] Bioengineering R&D Center Kragujevac, Kragujevac, Serbia
[3] University of Toronto, Toronto, Canada
[4] Methodist Hospital Research Institute, Houston

Abstract

High-gradient magnetic separation (HGMS) has attracted considerable attention in recent time, both experimentally and theoretically. It has established itself as a powerful technique for the manipulation of particles with magnetic properties. In the present study, analytical and numerical analysis of magnetic separation of cardiomyocytes (CMs) is presented. These enriched cells can be used for therapeutic or tissue engineering applications where no "labeling" method is accepted. Calculation of applied magnetic force for these particles that can be rendered as paramagnetic inside column was performed in order to clarify the effect of magnetic field gradient on the accumulation possibility of these particles. Numerical solutions of 2D fluid-structure finite element methods are compared with semi-analytical results for combination of magnetic field strength and average flow.

Keywords: cardiomyocytes, hearth failure, separation, magnetic force, paramagnetic,numerical simulations, finite element method

1. Introduction

Chronic cardiovascular disease such as heart failure is increasing to epidemic levels, affecting 1 in 5 persons. The beating heart muscle has no significant ability to regenerate and the viable tissue remaining after an injury such as myocardial infarction is often insufficient to maintain adequate cardiac output [Soonpaa and Field 1998]. Heart transplant very often is not available or appropriate option. Thus there is a pressing need for alternative interventions [Laflamme and Murry 2005] through innovative therapeutic solutions enabled by tissue engineering. Since cardiomyocytes (CM), the beating cells of the heart, are terminally differentiated, they cannot be propagated from the heart biopsies of adult patients. Recent advances in stem cell field enable deriving CMs from embryonic stem cells (ESCs) or induced pluripotent stem cells (iPSCs). However, engineering advances are required to enable label-free separation of these cells from heterogeneous populations in a cost-effective manner.

Proper methods for the separation of CMs, derived from ESC or iPSC are critical for the success of any therapeutic tissue engineering approach since the presence of undifferentiated cells can lead to teratoma formation upon implantation. Isolation methods that rely on inherent

physical properties of cells have been used for label-free separation of cells. For example [Murthy et al.] used a sieve-like microfluidic device to demonstrate the feasibility of enriching fibroblasts from cardiomyocytes on the basis of size. The high purity enrichment of CM from other cell types such as fibroblasts (FB) remains challenging because of the dimensional similarity of the suspended CMs to other cell types.

Amongst all inherent physical properties of cells for isolation purposes, perhaps the most relevant for cardiomyocytes are magnetic properties. Magnetic separation using high gradient magnetic separation method has been successfully implemented for the identification and isolation of red blood cells (RBCs) by taking advantage of the high level of iron in hemoglobin. Generally, much research [Watson and Phys 1973, Birss et al. 1976, Uchiyama et al. 1976, Uchiyama et al. 1977, Delatour et al. 1983, Gerber1984] has focused on developing magnetic separators based on this methodology because of the benefits such as the capacity to produce a large separation force with simple device structures, the low cost, ease of implementation. One of the problems on HGMS is lack of the methodology of designing the magnetic field strength and gradient. It is necessary to generate the strong magnetic field and magnetic gradient at the region from the magnet.

Here, an accumulation aspect in a microfluidic approach for label-free magnetic separation of cardiomyocytes (CMs) is presented. The basis for the separation is the higher amount of iron in CMs found in myoglobin (Mb) when compared to the iron level of other cardiovascular cells. After collagenase digestion, the heart isolate consists of CMs, fibroblasts (FB), smooth muscle cells (SMC) and endothelial cells (EC). The ratio of these cells in the native neonatal rat heart after collagenase digestion, as an example, is 47% CM, 48% FB, 3%SMC and 2% EC [Radisic et al. , Qiu et al. 1998]. Myoglobin (Mb) is found in both CM and SMC. However, the Mb content in SMC (~0.2mg/g wet weight) is significantly smaller than in CM (2.6-5.4mg/g wet weight), due to the high demand for oxygen in contracting CMs.

The accumulation of the paramagnetic particles in the column (CMs can be rendered as paramagnetic by treating the cells with a solution of $NaNO_2$ for a certain amount of time) and the magnetic force are estimated by calculation and modeling techniques. In order to clarify the effect of strong magnetic field gradient on the accumulation possibility of the magnetic particles, the numerical model system where the magnet was externally placed was used and the accumulation test was achieved.

2. Microfluidic device for the separation studies

In the device, nickel wire was wrapped around the circumference of a separation column. The column was placed in a vertical position between the permanent magnets with the flow inlet at the bottom of the column. The device captures the gravity, hydrodynamics and magnetic properties of the cells such that upon application of the field, paramagnetic cells remained in the column while non-magnetic cells (fibroblasts and other non-myocyte) traveled out of the column. The columns were fabricated by embedding a core inside PDMS (polydimethylsiloxane). The core was made by wrapping a nickel wire of thickness 69 um in diameter around a stainless steel rod. The rod was coated by an anti-sticking Teflon spray (Dupont) before the wrapping of the Nickel wire.

To generate uniform magnetic field four Neodymium-iron-boron permanent magnets of cubic shape (0.5”x0.5”x0.5”) were separated from 4 similar magnets by means of two spacers. In initial studies, it was observed that:

- The column diameter is 700 μm; length of column is 15mm.

- The field strength within the space was measured 0.2 to 2T.
- The average flow is between 2 and 20 μl/min.

3. Calculation of the trajectory of a paramagnetic particle in a cylindrical tube

In order to describe the motion of a small paramagnetic particle travelling in a fluid stream in the presence of a magnetized wire, one of assumes is that the particle experiences magnetic, hydrodynamic and gravitational forces. The balance of forces which describes the particle motion is given by eq. (1):

$$\vec{F} = \vec{F}_m + \vec{F}_D + \vec{F}_g + \vec{F}_b \tag{1}$$

whereF_m is magnetic force, F_g - gravitational force, F_b −buoyancy, and F_D - the drag force. The magnetic force $F_m$acting on a magnetic particle is proportional to the applied magnetic field H and magnetic field gradient ∇H:

$$F_m = \mu_0 V_p \chi_p H \nabla H \tag{2}$$

$\mu_0$is the magnetic permeability of free space, $V_p$is the particle volume, and $\chi_p$is the particle susceptibility. Since $F_m$depends directly on ∇H, high magnetic fields must be created in order to obtain a high magnetic force. This is especially true for micro-sized particles, since the magnetic force also depends on the cubic distance between the particle and wire axis [Svoboda 2004]. In order to clarify the value of magnetic force F_m required for accumulation, but also the value of average flow, the trajectory of magnetic particle flowing in the column under the magnetic field gradient was calculated.

The general configuration of the particle motion problem and a 2D schematic of particle control system utilized for modeling the targeting of magnetic particle by the magnetic force arising from the magnet placed outside the column are represented in Fig. 1. [Iacob 2004]:

$$F_{mr} = \frac{-\mu_0 k V_p M_s a^2}{r^3}\left(\frac{M_s a^2}{r^2} + H_0 \cos 2\theta\right) \tag{3}$$

$$F_{m\theta} = \frac{-\mu_0 k V_p M_s H_0 a^2}{r^3} \sin 2\theta \tag{4}$$

$$F_g = \rho_p g V_p \tag{5}$$

$$F_b = \rho_f g V_p \tag{6}$$

$$F_D = 6\pi c \eta \left(v_f - v_p\right) \tag{7}$$

where $k = \chi_p - \chi_f$ is difference of susceptibility of the particles (here CMs) and media at room temperature, r is distance of particle from the wire, a is wire radius, M_s saturation magnetization of wire, H_0 external magnetic field strength, η dynamic viscosity of fluid and $v_{f,} v_p$ represent the velocity of the fluid and the particle.

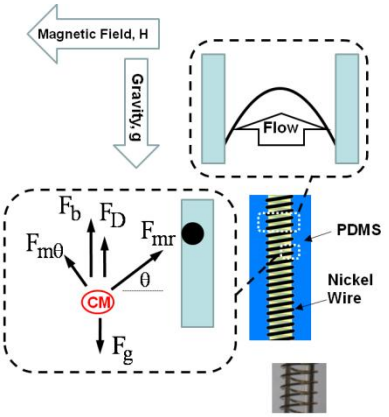

Fig. 1. Configuration of the particle motion problem and a 2D schematic of particle control system

The trajectory of the paramagnetic particle, positioned at the center of the column, is calculated using equations (3), (5), (6) and (7) since we treated paramagnetic cell that is at the same level as the nickel wire ($\theta = 0$).
When we initially set the magnetic particle in the cylindrical tube with a velocity defined as an initial velocity $v_0 = v(S_0)$ at the location $S_0[X_0, Y_0]$, a particle acceleration, $A_0 = A(S_0)$ at the $S_0[X_0, Y_0]$ is calculated using the equation (8)

$$\vec{A} = \frac{\vec{F}}{m_p} \tag{8}$$

where$m_p$is a mass of the magnetic particle. The second position, velocity, and acceleration are calculated using the equations (9), (10) and (11):

$$S_2 = S_1 + V_1 \cdot t + \frac{1}{2} A_1 \cdot t^2 \tag{9}$$

$$V_2 = V_1 + A_1 \cdot \mathrm{t} \tag{10}$$

$$A_2 = A(S_2) \tag{11}$$

Therefore, the nth position, velocity and acceleration of the particle after the running of rinsing flow are calculated using the following recurrent formulas (12), (13) and (14):

$$S_n = S_{n-1} + V_{n-1} \cdot t + \frac{1}{2} A_{n-1} \cdot t^2 \tag{12}$$

$$V_n = V_{n-1} + A_{n-1} \cdot \mathrm{t} \tag{13}$$

$$A = A(S_{n-1}) \tag{14}$$

4. Simulations results of the trajectory of the paramagnetic particles

In order to realize how strong magnetic field is needed to accumulate the paramagnetic particle on the wall of the column, the calculated particle trajectories for different magnetic field strengths for constant average flow are shown on Fig. 2. For example, when we apply the magnetic field greater than 1T for average flow of 5μl/min, a particle can be easily

accumulated on the wall. Also, the greater average flow, the greater magnetic field is needed to attract the particle toward the column wall.

Simultaneously, this Figure can give us the information after how long distance the cell at the centerline of column will be accumulated on the column wall in the presence of flow. If this paramagnetic cell stay trapped in the column, general conclusion is that all cells from the bottom of the column for these parameters remain in the column. But, one of the challenging tasks is to define which percentage of cells stay in the column if the observed cell leave the column. These values are represented in Table 1.

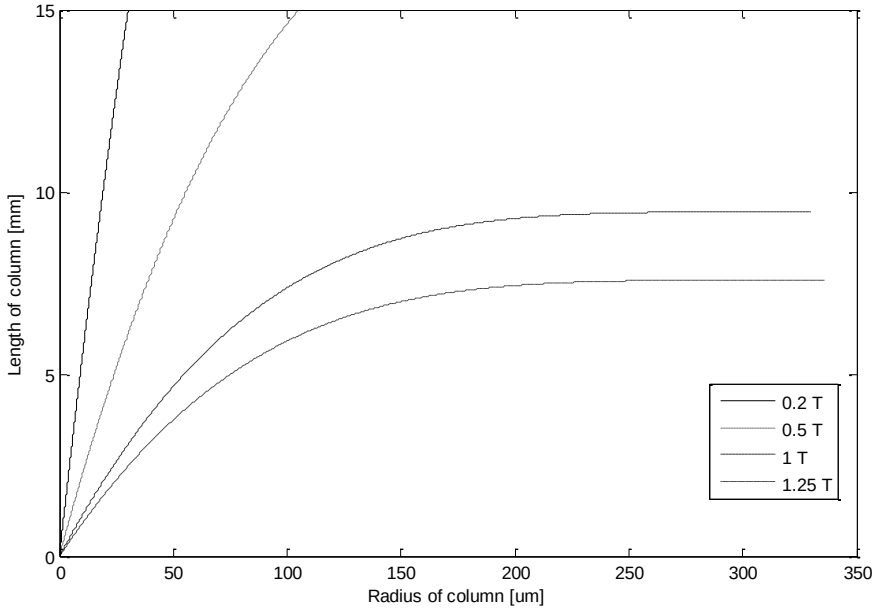

Fig. 2. The calculated particle trajectory under different magnetic field strength (average flow: $5\frac{\mu l}{\min}$, $B = 0.2T, 0.5T, 1T, 1.25T$). Y-axis is a displacement in flow direction from the initial position to the final position within the column. X-axis is a displacement from the center of the column to the wall

Magnetic field strength [T]	Displacement along Y-axis [mm]	Percentage of trapped cells
0.2	Cell will leave the column	75%
0.5	Cell will leave the column	75%
1	9.452	100%
1.25	7.577	100%

Table 1. Analytical results for maximal length for deposition of particles and percentage of trapped cells

According to experiment, uniform magnetic field is formed by four Neodymium-iron-boron permanent magnets of cubic shape (0.5"x0.5"x0.5") that were separated from 4 similar magnets by means of two spacers so that the field strength within the space was measured at 1.25T. In that case, our goal was to define flow where the particle will be accumulated in the column. It can be seen in the Fig. 3., that flow must be lower than 9.5μl/min.

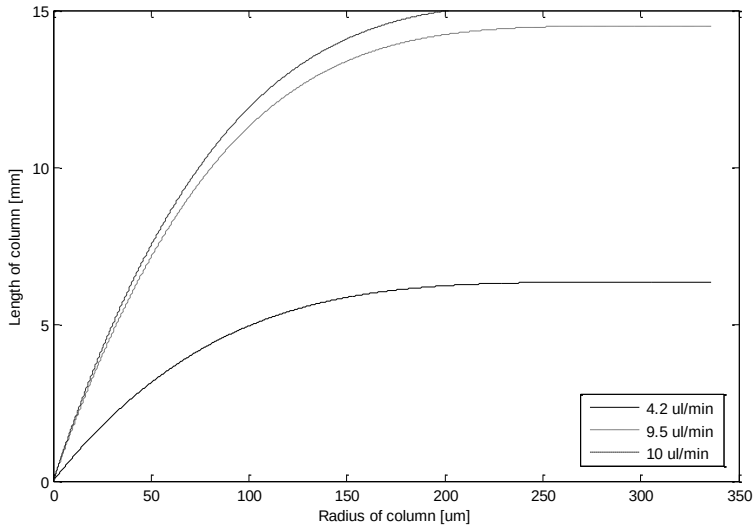

Fig. 3. The calculated particle trajectory under fluid flow (magnetic field strength: 1.25 T). Y-axis is a displacement in flow direction from the initial position to the final position within the column. X-axis is a displacement from the center of the column to the wall. 1) at 4.2μL/min, the cell will fall on the column wall after 6.345mm and percentage of trapped cells is 100% for a column described in this paper which is 15 mm long; 2) at 9.5 μL/min, the cell will fall on the column wall after 14.508mm and percentage of trapped cells is 100%; 3) at 10 μL/min, this cell will leave the column, percentage of trapped cells is 75%

The parameters used for calculating the particle trajectory are summarized in Table 2.

Variable	Name	Value	Unit
μ_0	Vacuum permeability	$4\pi \times 10^{-7}$	H/m
k_p	Magnetic susceptibility of Cell (neonatal rat)	1.58×10^{-5}	
k_f	Magnetic susceptibility of fluid	-0.9×10^{-5}	
a	Nickel wire radius	34.5	μm
M_S	Saturation Magnetization of Nickel	486×10^3	A/m
r	Distance of cell from the wire	0-350	μm
B_0	External magnetic Field	1.25	T
g	Gravity	9.81	m/s2
θ	Angle to define the location of cell vs wire		Rad
η	Dynamic viscosity of fluid	0.001	Ns/m2
ρ_p	CM density	1060	kg/m3
ρ_f	Fluid density	1000	kg/m3
C	Radius of cell (neonatal rat)	7	μm

Table 2. Parameters of the analytical study

5. Numerical methods for finite element simulation

For numerical modeling of body motion in fluids we use finite element method. Particle motion is described with the Newton`s motion equation,fluid domain is described with the Navier – Stoke`s equations and magnetic field with additional external force.

Coupling equations of the solid and fluid is achieved by kinematic condition of velocity equality in the nodes on the interfacebetween fluid and solid. This condition is achieved by generating a fluid mesh at each time step and by interpolating last known solution on fluid mesh nodes.

The equations of motion of the material system can be written by applying the principle of virtual work, taking into account the effect of inertial forces. The principle of virtual work expresses the equality of virtual work of internal and external forces.

$$\delta W_{\text{int}} = \delta W_{ext} \tag{15}$$

Where are:

$$\delta W_{\text{int}} = \int_V \delta \mathbf{e}^T \boldsymbol{\sigma} dV \tag{16}$$

$$\delta W_{ext} = \int_V \delta \mathbf{u}^T \left(\mathbf{F}^V - \rho \ddot{\mathbf{u}} \right) dV + \int_{S^\sigma} \delta \mathbf{u}^T \mathbf{F}^S dV + \sum_i \delta \mathbf{u}^T \mathbf{F}^{(i)} \tag{17}$$

virtual work of internal and external forces. Physical quantities in equations 16 and 17 are:

$\mathbf{e}$ - strain tensor,

$\boldsymbol{\sigma}$ - stress tensor,

$\mathbf{u}$ - displacement vector,

ρ - density,

$\ddot{\mathbf{u}}$ - acceleration vector

$\mathbf{F}^V$, $\mathbf{F}^S$, $\mathbf{F}^{(i)}$ - Volume, surface and concentrated external force.By using constitutive relations for linear elastic material and introducing isoparametric interpolation functions for displacements, the equations of motion of materials systems in discrete form are:

$$\delta \mathbf{U}^T \int_V \left(\mathbf{B}^T \mathbf{C} \mathbf{B} dV \right) \mathbf{U} + \delta \mathbf{U}^T \int_V \left(\mathbf{N}^T \rho \mathbf{N} dV \right) \ddot{\mathbf{U}} = \delta \mathbf{U}^T \mathbf{F} \tag{18}$$

or:

$$\mathbf{M}\ddot{\mathbf{U}} + \mathbf{K}\mathbf{U} = \mathbf{F} \tag{19}$$

where:

$\mathbf{K} = \int_V \mathbf{B}^T \mathbf{C} \mathbf{B} dV$ - element stiffness matrix,

$\mathbf{M} = \int_V \mathbf{N}^T \rho \mathbf{N} dV$ - mass matrix elements.

The equation (19) can be written in the incremental form:

$$\mathbf{M}\ddot{\mathbf{U}} + {}^{t+\Delta t}\mathbf{K}^{(i-1)} \Delta \mathbf{U}^{(i)} = {}^{t+\Delta t}\mathbf{F}_{ext} - {}^{t+\Delta t}\mathbf{F}_{int} \tag{20}$$

where:

${}^{t+\Delta t}\mathbf{F}_{int}^{(i-1)} = \int_V {}^{t+\Delta t}\mathbf{B}^{T(i-1)\,t+\Delta t}\boldsymbol{\sigma}^{(i-1)} dV$ - vector of internal forces in the last known configuration, at the end of load step.

Since the fluid flow is described by the Navier - Stokes equations, where unknown values are velocity and pressure, it is suitable to transform equation (6) in that way so the velocity field is unknown. We believe that the acceleration in the time step is constant and can be expressed as the velocity increment in the current step:

$$ {}^{t+\Delta t}\ddot{\mathbf{U}}^{(i)} = \frac{{}^{t+\Delta t}\dot{\mathbf{U}}^{(i)} - {}^{t}\dot{\mathbf{U}}}{\Delta t} \tag{21} $$

Displacement increment can be expressed as a product of velocity increment in the current step and the time step duration:

$$ \Delta\mathbf{U}^{(i)} = \Delta\dot{\mathbf{U}}^{(i)} \cdot \Delta t \tag{22} $$

Substituting equation (21) and (22) in equation (20), we get the final form of solid motion equations:

$$ \left(\frac{\mathbf{M}}{\Delta t} + {}^{t+\Delta t}\mathbf{K}^{(i-1)}\,\Delta t \right) \Delta\dot{\mathbf{U}}^{(i)} = {}^{t+\Delta t}\mathbf{F}_{ext} - \mathbf{F}_{int}^{(i-1)} - \frac{\mathbf{M}}{\Delta t}\left({}^{t+\Delta t}\dot{\mathbf{U}}^{(i-1)} - {}^{t}\dot{\mathbf{U}} \right) \tag{23} $$

As already mentioned, to describe fluid flow Navier Stokes equations are applied:

$$ \begin{bmatrix} \frac{1}{\Delta t}\mathbf{M} + {}^{t+\Delta t}\hat{\mathbf{K}}_{vv}^{i-1} & \mathbf{K}_{vp} \\ \mathbf{K}_{vp}^{T} & \mathbf{0} \end{bmatrix} \begin{Bmatrix} \Delta\mathbf{V}^{i} \\ \Delta\mathbf{P}^{i} \end{Bmatrix} = \\ \begin{Bmatrix} {}^{t+\Delta t}\mathbf{F}_{ext}^{i-1} \\ \mathbf{0} \end{Bmatrix} - \begin{bmatrix} \frac{1}{\Delta t}\mathbf{M} + {}^{t+\Delta t}\mathbf{K}_{vv}^{i-1} & \mathbf{K}_{vp} \\ \mathbf{K}_{vp}^{T} & \mathbf{0} \end{bmatrix} \begin{Bmatrix} {}^{t+\Delta t}\mathbf{V}^{i-1} \\ {}^{t+\Delta t}\mathbf{P}^{i-1} \end{Bmatrix} + \begin{Bmatrix} \frac{1}{\Delta t}\mathbf{M}\,{}^{n}\mathbf{V} \\ \mathbf{0} \end{Bmatrix} \tag{24} $$

The unknown values per nodes are velocity and pressure. Equation (24) is derived using mixed V-p formulations.

Some of the results for different fluid flow boundary conditions are presented in Fig. 4. Solid domain contained 121 nodes and 100 four node elements. Fluid domain has 1500 nodes and 1300 elements. Input flows are Q = 4.2 , 20, 50, 144 μl/min and corresponding time steps are: dt = 3.0e-3, 1.0e-3, 5.0e-4, 1.0e-4 s. Applied magnetic force is the same as it is described in section 4. Difference in the results from 2D fluid-structure finite element method and analytical method are due to different formulation. Analytical solution assumes 3D conditions and numerical 2D. Future research are necessary to compare these two methods.

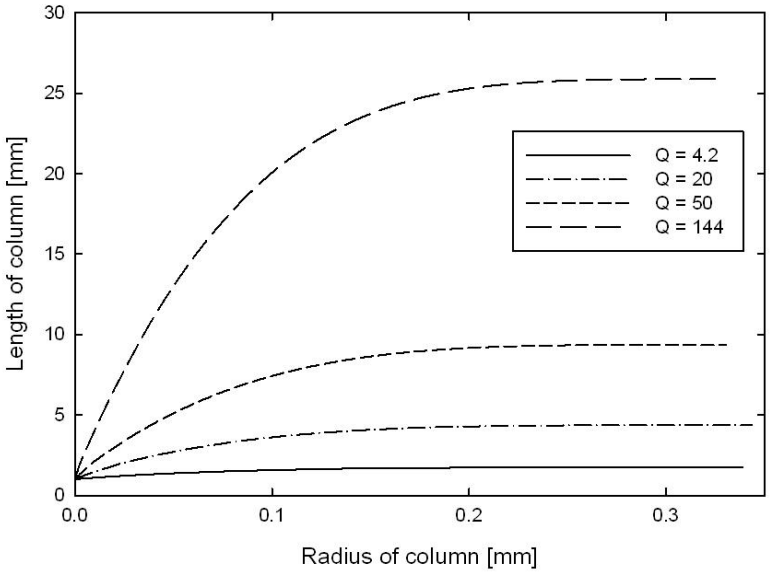

Fig. 4. Trajectories for 2D numerical simulation using fluid-structure interaction method for different fluid inflow boundary condition

The yield of the process in experiments presented in this paper is limited by the capacity of the column. Loading the cells with too concentrated cell mixture would result in the rinsing of CM, and consequently losing cells. It was observed that maximum yield of over 80% was achieved when the total cell number that was loaded into the column was less than 10000. At each experiment between 3000-5000 adult CM was collected. Using only one column and given that each experiment takes 30 minutes the through-put of the experiments in this study was between 6000-10000 collected cardiomyocytes/hour.

Comparison between numerical and experimental results for the inlet flows of 4.2, 20, 50 and 144μl/min is presented in Table 3. It can be observed that good accuracy was achieved for these experimental conditions.

Q [**μl/min**]	Numerical maximal length [mm]	Experimental maximal length [mm]
4.2	1.86	2.0
20	4.63	5.0
50	9.34	9.0
144	26.45	27.0

Table 3. Comparison between experimental and numerical results for maximal length of tube for deposition of the magnetic particles

6 Software

Calculations performed in calculation of particle deposition arequite demandingfrom the aspect of computer hardware requirements and calculation time. In order to overcome those lacks browser hosted application for running simulations on the server machines, remotely, is developed. Application was conceived in a way that user can easily access to the application, via web browser, set necessary parameters, run calculation on remote computer and visualize results after calculation completion.

Application is developed using the two actual Microsoft technologies. WPF -windows presentation foundation for creating rich user-friendly browser hosted application Fig. 5, and WCF - windows communication foundation for communication between client and server computer.

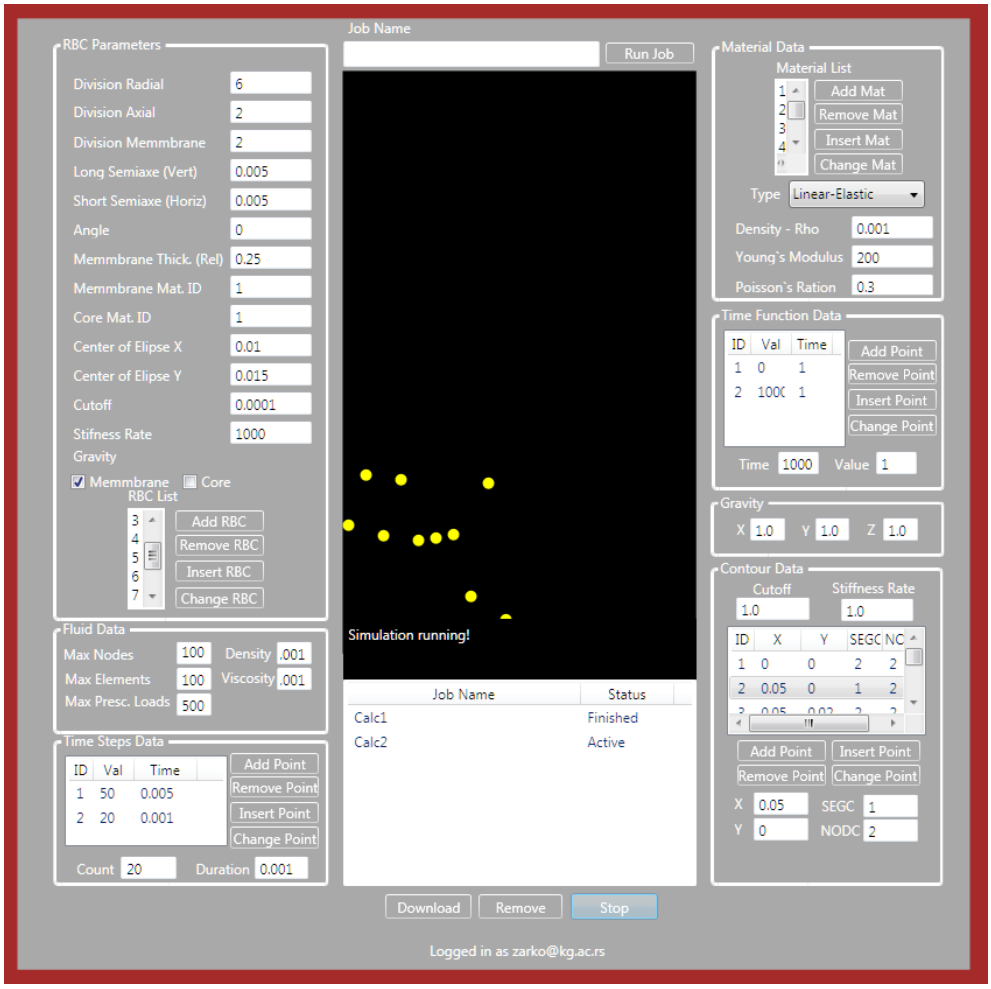

Fig. 5. Browser hosted application

WCF is Microsoft's platform for building distributed service-oriented applications for the enterprise and the web that are secure, reliable, and scalable [Leroux 2009]. WCF Scenarios that were used are:

- Classic client-server applications where clients access functionality on remote server machines
- Distribution of services behind the firewall in support of a classic service-oriented architecture
- Asynchronous or disconnected calls implemented with queued messaging patterns
- Workflow services for long running business operations

In order for a client to call operations, exposed by a hosted service, he has to access service metadata (the contract) to send messages with the required parameters, and process return values accordingly. In our application service`s task is to process client`s requests, together with calculations parameters and to manage execution of preprocessing unit and finite element solver. Beside previously mentioned any additional client service communication, such as monitoring calculation progress, data validation, user authentication, etc. is achieved by two-way communication between service and client. Benefits of two-way communication is obtained by employing duplex message exchange pattern in which both endpoints can send messages to each other independently. A duplex service, therefore, can send messages back to the client endpoint, providing event-like behavior which only works within a session.

In order to create a duplex contract we created a pair of interfaces. The first is the service contract interface that describes the operations that a client from browser-hosted application can invoke. That service contract must specify a *callback contract, Fig. 6*. The callback contract is the interface that defines the operations that the service can call on the client endpoint. A duplex contract does not require a session, although the system-provided duplex bindings make use of them.

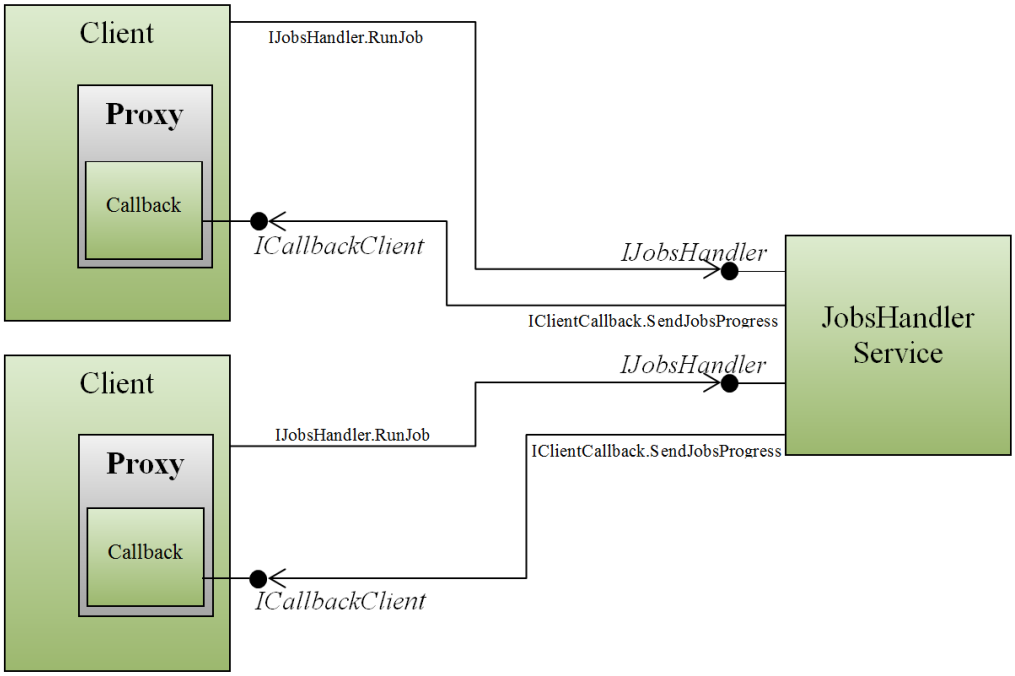

Fig. 6. Duplex message exchange pattern

7. Conclusion

In this study analytical and numerical analysis of magnetic separation of cardiomyocytes is presented. Magnetic field gradient is used to see the effect of on the accumulation possibility of particles inside the column with paramagnetic cells. Analytical and numerical solutions are compared for combination of magnetic field strength and average flow where all the particles were in the column. Due to large scale numerical calculations specific software for parallel computing on the server machine remotely was developed. Obtained results can be used for better optimization and design of the device for magnetic separation of cardiomyocytes in the biomedical tissue engineering.

Извод

Аналитичка и нумеричка анализа магнетне сепарације кардиомиоцита

B.Cirkovic[1],V.Isailovic[2], Z.Milosevic[2], J.Radulovic[1], A.Sofla[3], M.Radisic[3], M.Kojic[2,4], N.Filipovic[1,2]

[1] Faculty of Engineering, University of Kragujevac, Kragujevac, Serbia
[2] Bioengineering R&D Center Kragujevac, Kragujevac, Serbia
[3] University of Toronto, Toronto, Canada
[4] Methodist Hospital Research Institute, Houston

Резиме

Магнетна сепарација са великим градијентом у последње време привлачи велику пажњу, са аспекта експеримената и теорије. Показала се као веома моћна техника за манипулацију ћелијама са магнетним особинама. У данашњим истраживањима, веома је актуелна аналитичка и нумеричка анализа магнетне сепарације ћелија кардиомиоцита. Ове обогаћене ћелије имају терапеутску примену као и примену у инжењерингу ткива где су прихваћене методе без обележавања. Прорачуни магнетне силе је извршен са циљем да се разјасни утицај градијента магнетног поља на таложење ћелија. Нумеричка решења методе коначних елемената за дводимензионални случај су поређене са полу-аналитичким резултатима за различите комбинације јачине магнетног поља и протока флуида.

Кључне речи: кардиомиоцити, отказивање срца, сепарација, магнетна сила, парамагнетичан, нумеричке симулације , метод коначних елемената

References

C. Delatour, G. Schmitz, E. Maxwell and D. Kelland, IEEE Trans. Magn., 1983, MAG-19, 2127–2129.

Dimmeler, S., A.M. Zeiher, and M.D. Schneider, Unchain my heart: the scientific foundations of cardiac repair. J Clin Invest, 2005. 115(3): p. 572-83.

Gh. Iacob, O. Rotariub,N.J.C. Strachan b and U.O. Häfeli, "Magnetizable needles and wires – modeling an efficient way to target magnetic microspheres in vivo", Biorheology 41 (2004), 599–612.

J. H. P. Watson, J. Appl. Phys., 1973, 44, 4209.

J. Svoboda, "Magnetic Techniques for the Treatment of Materials", Kluwer Academic Publishers, Dordrecht, the Netherlands. 2004.

Laflamme, M.A. and C.E. Murry, Regenerating the heart. Nat Biotechnol, 2005. 23(7): p. 845-56.

Michele Leroux Bustamante, WCF Guidance for WPF Developers, May 2009.

Qiu Y, Sutton L, Riggs AF. Identification of myoglobin in human smooth muscle. J Biol Chem 1998;273:23426-23432.

R. Gerber, IEEE Trans. Magn., 1984, MAG-20, 1159–1164.
R. R. Birss, R. Gerber and M. R. Parker, IEEE Trans. Magn., 1976, MAG-12, 892–894.
Radisic M, Park H, Martens TP, Salazar-Lazaro JE, Geng W, Wang Y, Langer R, Freed LE, Vunjak-Novakovic G. Pre-treatment of synthetic elastomeric scaffolds by cardiac fibroblasts improves engineered heart tissue. J Biomed Mater Res A In press.
S. Uchiyama, S. Kondo and M. Takayasu, IEEE Trans. Magn., 1976, MAG-12, 895–897.
S. Uchiyama, S. Kurinobu, M. Kumazawa and M. Takayasu, IEEE Trans. Magn., 1977, MAG-13, 1490–1492.
Shashi K. Murthy · Palaniappan Sethu ·Gordana Vunjak-Novakovic · Mehmet Toner ·Milica Radisic, Size-based microfluidic enrichment of neonatal rat cardiac cell populations.
Soonpaa, M.H. and L.J. Field, Survey of studies examining mammalian cardiomyocyte DNA synthesis. Circulation Research, 1998. 83(1): p. 15-26.